

# DIAGNOSIS OF TRANSVERSE EMITTANCE IN LASER-DRIVEN ION BEAM

T. Miyatake<sup>1</sup>, H. Sakaki<sup>1</sup>, I. Takemoto<sup>1</sup>, Y. Watanabe, Kyushu University, Kasuga, Hukuoka, Japan

T. H. Dinh, S. Kojima, Ki. Kondo, Ko. Kondo, M. Kando, M. Nishikino, M. Nishiuchi, National Institutes for Quantum and Radiological Science and Technology KPSI, Kizugawa, Kyoto, Japan

<sup>1</sup>also at National Institutes for Quantum and Radiological Science and Technology KPSI, Kizugawa, Kyoto, Japan

## Abstract

Ion beam produced in laser-driven ion acceleration by ultra-intense lasers has characteristics of high peak current and low emittance. These characteristics become an advantage to operate the request for the beam application. Therefore, we study how to control the parameters with the laser-plasma interaction.

Here, we used 2D Particle-in-Cell code to simulate the laser-driven ion acceleration and investigated the results in terms of transverse emittance, beam current, and brightness. The laser spot size and target thickness were changed in the simulation. And, these qualitative results show that interaction target thickness is a major factor in controlling beam characteristics.

## INTRODUCTION

A laser-driven ion acceleration by ultra-intense lasers [1-3] is expected to be applied to various applications such as down-size of particle accelerators, hadron therapy [4], and physical property experiments including PIXE [5, 6]. In the Target Normal Sheath Acceleration (TNSA) scheme which is a well-known mechanism of laser-driven acceleration, an ultra-intense laser is focused on a solid thin foil target to accelerate electrons, and generate a charge-separating electric field gradient of  $\sim$ TV/m. This field accelerates ionized hydrogen, carbon, and oxygen in a contaminant layer on the rear side of a target in  $\sim$ MeV. The transverse proton emittance diagnosis is smaller than 0.004 mm-mrad (normalized RMS value) for 10 MeV protons [7], and the emittance of the laser-accelerated proton beam is much lower than that of existing RF accelerators [8, 9]. An emittance growth of the accelerated proton beam is discussed by Andreas J. Kemp *et al.*, that is caused by the filamentation of the laser-generated hot-electron jet [10].

Low emittance and high peak current, high-quality beam, become an advantage to operate the request for the beam application. Therefore, we study how to control the parameters with the laser-plasma interaction which is to clarify the correlation between laser irradiation parameters and beam characteristics of laser-accelerated ions. To understand these correlations, we can optimize the conditions for generating a high-quality beam. Generally, such as emittance and current are estimated analytically from the plasma density of an ion source and conditions of the extraction electrode [11, 12] in a typical ion source, ECR

source. However, it is not easy to make an analytical model such as typical accelerator ion source for the laser-accelerated ion beams. In this paper, we systematically diagnose the correlation between laser parameters and generated beam quality.

## PARTICLE-IN-CELL SIMULATION

An ideal beam is close to zero transverse emittance, but a real beam has a non-zero emittance generated while laser-plasma interaction process. We have to understand the contributing factors to control the beam quality such as emittance and beam current. Here, we focus on and evaluate two contributing factors, interaction target thickness and spot size of a laser as shown in Fig. 1.

Generating of low emittance and high peak current proton beams in TNSA scheme is simulated with a 2D Particle-in-Cell (PIC) code, EPOCH code version 4.17.10 [13], by changing a target thickness and spot size of a laser. To simplify the analysis, it is assumptive to collisionless in the simulation conditions. The diagnostic divergence angle is limited to  $\pm 50$  mrad, due to the aperture of the beam transport system [9, 14]. The proton beam energy to be observed is 2 MeV with  $\pm 5\%$  energy dispersion. The dimensions of the simulation box are  $80\ \mu\text{m} \times 80\ \mu\text{m}$  and the cell size is  $0.042\ \lambda_L \times 0.042\ \lambda_L$  where  $\lambda_L$  is the laser wavelength. The laser has linearly polarized. The laser spatial distribution is assumed to be a single Gaussian distribution which is a longitudinal profile with 80 fs (FWHM). The electron density of target is set to  $n_e = 40\ n_c$ , where  $n_c = \epsilon_0 m_e \omega^2 / e^2$

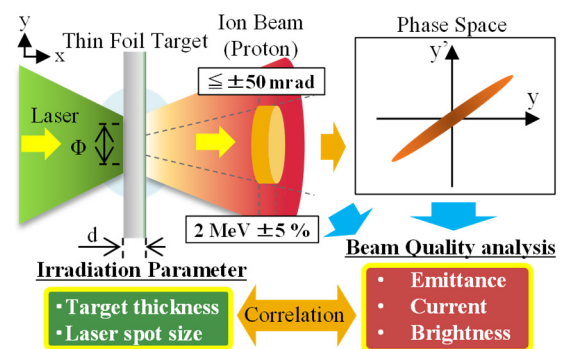


Figure 1: Overview of the calculation scheme. The phase space is created to calculate the emittance,  $d$  is the target thickness, and  $\phi$  is the laser spot diameter.

is the electron critical density,  $\epsilon_0$  is the vacuum permittivity,  $\omega$  is the laser frequency, and  $m_e$  and  $e$  are the electron mass and charge, respectively. The target is composed of polyimide and 20 nm thick contaminant on the rear-side of the target. The polyimide layer is defined as carbon to proton number ratio of 2:1 and the contaminated layer as a pure proton layer. The pre-plasma produced by the laser pre-pulse is set up with an exponential density distribution on the plane of incidence of the laser and a scale length ( $L = 4\lambda_L$ ).

This simulation is to evaluate the beam emittance, current, and brightness in the simulation for each laser irradiation condition at 1000 fs after the laser-plasma interaction. The normalized rms emittance in simulation  $\epsilon_{SimNR}$  is calculated using equation (1), which is determined by the transverse space  $x$  and angle  $x'$  [15].

$$\epsilon_{SimNR} = \gamma\beta\sqrt{\langle x^2 \rangle \langle x'^2 \rangle - \langle xx' \rangle^2} \quad (1)$$

Where  $\langle \rangle$  is the average value. In this paper, the beam pulse widths at 3  $\mu\text{m}$  and 12  $\mu\text{m}$  thickness were compared, and these have about 100 fs in both cases, and the difference of pulse width was only a few percent. Since this difference does not significantly affect the beam current, the pulse width is assumed to be uniform. So, the beam current in simulation  $I_{Sim}$  is defined as an amount of charge divided by a beam pulse width of 100 fs. We use Brightness as a unit to express the beam quality. The brightness in simulation  $B_{Sim}$  is defined arbitrarily as beam current divided by the square of the emittance as in equation (2).

$$B_{Sim} = I_{Sim} / \epsilon_{SimNR}^2 \quad (2)$$

Note that the values obtained from these calculations are arbitrary quantities defined in the simulation and are not quantitatively comparable to experimentally measured values.

## SIMULATION RESULTS

### Brightness Variation with Target Thickness Scanning

Brightness is compared with respect to the target thickness dependence. The laser spot size is 5  $\mu\text{m}$  (FWHM) and the focused intensity is  $6.5 \times 10^{18} \text{ W/cm}^2$ . Target thickness is scanned at 3, 5, 7.5, and 12  $\mu\text{m}$ . The phase space profiles of the proton beam for the target thickness of 3 and 12  $\mu\text{m}$  are shown in Fig. 2(a-b), respectively. These phase-space distributions consist of protons only within  $\pm 50 \text{ mrad}$ , and emittance is calculated from these distributions. The phase space distribution for the 12  $\mu\text{m}$  thickness shows a larger dispersion in  $y$ - $y'$  space than the 3  $\mu\text{m}$  results, and this difference affects the emittance. Figure 3 shows a two-dimensional brightness color map. The yellow circle shows the result of scanning the target thickness. The emittance value tends to increase for thicker targets as can be seen from Fig. 3. Comparing the 3  $\mu\text{m}$  and 12  $\mu\text{m}$  thicknesses, the emittance value for the 12  $\mu\text{m}$  increased by 202.0 % compared to the 3  $\mu\text{m}$ . The current in Fig. 3 shows a decreasing trend with increasing target thickness.

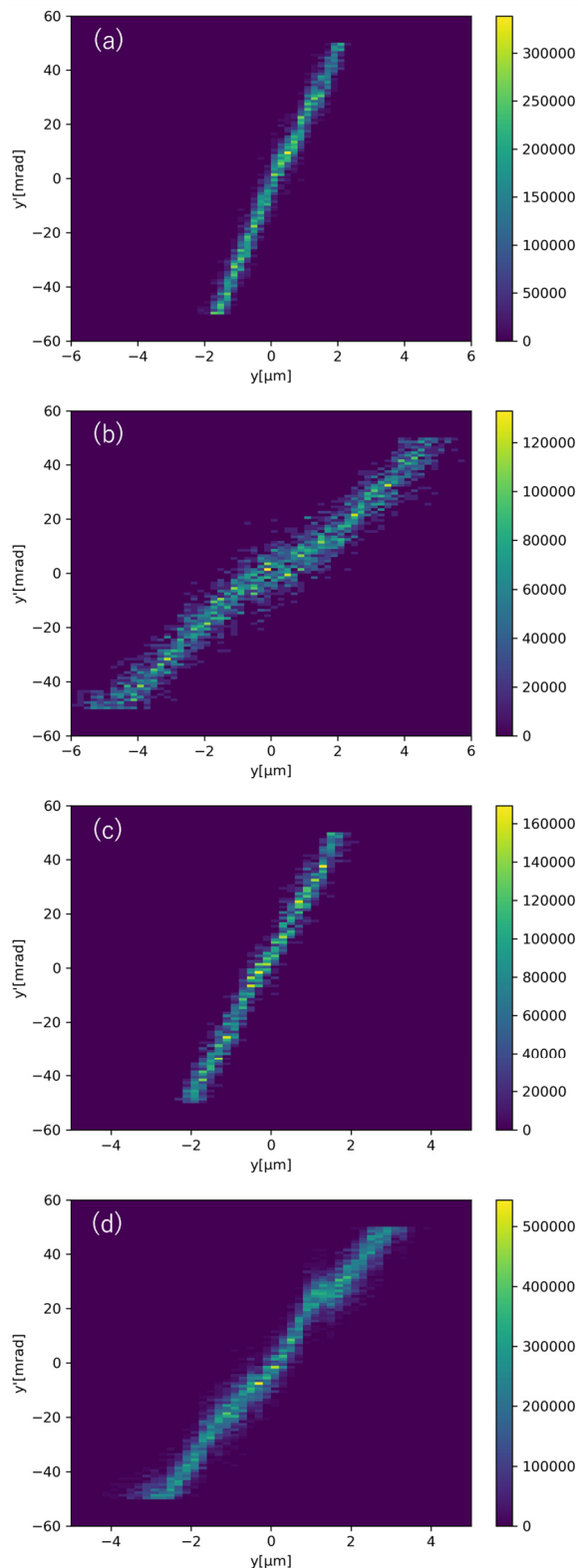


Figure 2: Transverse phase space profile of  $y$ - $y'$ . The energy of protons to be observed is 2 MeV with  $\pm 5\%$  dispersion. (a) and (b) show results for target thickness of 3 and 12  $\mu\text{m}$ , respectively, (c) and (d) show results for laser spot sizes of 3.5 and 10.0  $\mu\text{m}$ . A color bar shows a simulation particle number, and the color intensity is normalized from purple to yellow for each map.

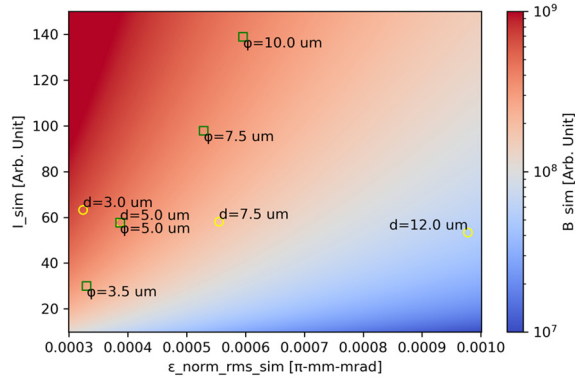


Figure 3: The distribution of brightness with red to blue color map. The horizontal axis is the normalized rms emittance and the vertical axis is the beam current in the simulation. "d=" indicates the thickness, and  $\phi$  indicates the laser spot diameter.

However, the current is reduced by only 15.6 % when comparing 3  $\mu\text{m}$  and 12  $\mu\text{m}$  thickness. The highest brightness is observed at a thickness of 3  $\mu\text{m}$ , which is more than an order of magnitude higher for the 3  $\mu\text{m}$  compared to the 12  $\mu\text{m}$ .

### Brightness Variation with Laser Spot Size Scanning

Brightness is also compared with respect to the laser spot size dependence. The target thickness is constant at 5  $\mu\text{m}$ . The spot radius is scanned at 3.5, 5, 7.5, and 10  $\mu\text{m}$  (FWHM), and the laser energy is adjusted so that the focused intensity is constant at  $6.5 \times 10^{18}$  W/cm<sup>2</sup>. The phase-space profiles of the proton beam for spot sizes of 3.5 and 10  $\mu\text{m}$  are shown in Fig. 2(c-d), respectively. The phase space distribution for the 10  $\mu\text{m}$  spot size shows a slightly larger dispersion in y-y' space than the 3.5  $\mu\text{m}$  result. The correlations between emittance and current are shown in Fig. 3, and this brightness is plotted in the green square respectively. Figure 3 shows that both emittance and current show an increasing trend for larger spot size. The emittance increased by 80.7 % and the current increased by 363.4 % for the spot size of 10.0  $\mu\text{m}$  compared to the 3.5  $\mu\text{m}$ . In this case, the brightness increased by only 42.1 %.

### Discussion

The results of target thickness scanning show that controlling target thickness has a strong effect on the emittance change and has a little effect on the current. That is, target thickness has a strong influence on brightness. This difference in emittance is due to the spatial spreading and the increase in angular dispersion with increasing target thickness. It is clear from a comparison of the phase space distributions in Fig. 2 (a) and (b). These physical mechanisms are currently under investigation by detailed analysis such as EM field distribution and return current effect.

The results of spot size scanning show that spot size expansion increases both current and emittance. These results indicate that brightness is relatively insensitive to varies in a laser spot size. Irradiation with a large spot size is an

effective parameter for increasing current, but later stage applications must allow for large emittance. Note that irradiation with a larger spot size requires higher laser energy, making it more difficult to achieve a focused intensity. The above discussion concludes that target thickness is a suitable parameter for controlling beam quality. Other parameters, such as laser energy, also need to be characterized.

Also, the simulation assumed collisionless condition, and the particle density set in this simulation is small relative to the solid density in real. Due to these unconsidered phenomena, emittance and current are not quantitatively guaranteed. Since the proton energies to be analysed are in the plateau region, which is relatively lower than the peak energy of acceleration, the results may differ near the peak energy. The emittance growth continues after the 1000 fs observed in this simulation because there are nonlinear forces such as space-charge effects and charge-neutral effects of the electron cloud.

## CONCLUSION

We studied the correlation between laser irradiation parameters and beam quality using 2D particle-in-cell simulations, with the aim of optimizing the beam quality of laser-accelerated ions controllable. Simulated Ion beams were evaluated them using emittance, current, and brightness. The results show that target thickness is an effective parameter for controlling beam emittance. The characteristic that thinner targets produce beams with higher brightness was shown. In the future, we will conduct more detailed calculations, including collision effects and 3D-PIC simulations. The effects of the acceleration field and magnetic field on beam quality will be analysed. Experiments for measuring an emittance, a current, and a brightness to confirm the characteristics obtained from the simulations are in progress.

## ACKNOWLEDGEMENTS

This work was supported by JST-MIRAI R&D Program No. JPMJMI17A1.

This work was supported by JSPS KAKENHI Grant Number JP21J22132.

## REFERENCES

- [1] E. L. Clark *et al.*, "Measurements of Energetic Proton Transport through Magnetized Plasma from Intense Laser Interactions with Solids", *Phys. Rev. Lett.*, vol. 84, p. 670, 2000.
- [2] A. Maksimchuk, S. Gu, K. Flippo, D. Umstadter, and V. Y. Bychenkov, "Forward Ion Acceleration in Thin Films Driven by a High-Intensity Laser", *Phys. Rev. Lett.*, vol. 84, p. 4108, 2000.
- [3] R. A. Snavely *et al.*, "Intense High-Energy Proton Beams from Petawatt-Laser Irradiation of Solids", *Phys. Rev. Lett.*, vol. 85, p. 2945, 2000.
- [4] S. Bulanov, T. Esirkepov, V. Khoroshkov, A. Kuznetsov, and F. Pegoraro, "Oncological Hadrontherapy with Laser Ion Accelerators", *Phys. Lett. A*, vol. 299, pp. 240-247, 2002.

- [5] M. Barberio and P. Antici, “Laser-PIXE Using Laser-accelerated Proton Beams”, *Scientific Reports*, vol. 9, p. 6855, 2019.
- [6] M. Passoni, L. Fedeli and F. Mirani, “Superintense Laser-driven Ion Beam Analysis”, *Scientific Reports*, vol. 9, p. 9202, 2019.
- [7] T. E. Cowan *et al.*, “Ultralow Emittance, Multi-MeV Proton Beams from a Laser Virtual-Cathode Plasma Accelerator”, *Phys. Rev. Lett.*, vol. 92, p. 204801, 2004.
- [8] F. Nürnberg *et al.*, “Radiochromic Film Imaging Spectroscopy of Laser-accelerated Proton Beams”, *Rev. Sci. Instrum.*, vol. 80, p. 033301, 2009.
- [9] M. J. Wu *et al.*, “Emittance Measurement along Transport Beam Line for Laser Driven Protons”, *Phys. Rev. Accel. Beams*, vol. 23, p. 031302, 2020.
- [10] A. J. Kemp *et al.*, “Emittance Growth Mechanisms for Laser-accelerated Proton Beams”, *Phys. Rev. E*, vol. 75, p. 056401, 2007.
- [11] S. L. Chen and T. Sekiguchi, “Instantaneous Direct-Display System of Plasma Parameters by Means of Triple Probe”, *J. of Appl. Phys.*, vol. 36, p. 2363, 1965.
- [12] J. Ishikawa, F. Sano, and T. Takagi, “Ion Beam Extraction with Ion Space-charge Compensation in Beam-plasma Type Ion Source”, *J. of Appl. Phys.*, vol. 53, p. 6018, 1982.
- [13] T. D. Arber *et al.*, “Contemporary Particle-in-Cell Approach to Laser-Plasma Modelling”, *Plasma Physics Controlled Fusion*, vol. 57, p. 113001, 2015.
- [14] H. Sakaki *et al.*, “Prompt In-Line Diagnosis of Single Bunch Transverse Profiles and Energy Spectra for Laser-Accelerated Ions”, *Appl. Phys. Express*, vol. 3, p. 126401, 2010.
- [15] M. Zhang, “Emittance Formula for Slits and Pepper-pot Measurement”, *Fermi National Accelerator Lab. Technical Report*, vol. 28, p. 28018451, 1996.